Impacts of thermohaline circulation shutdown in the twenty-first century

Michael Vellinga · Richard A. Wood

Abstract We discuss climate impacts of a hypothetical shutdown of the thermohaline circulation ('THC') in the 2050s, using the climate model HadCM3. Previous studies have generally focussed on the effects on pre-industrial climate. Here we take into account increased greenhouse gas concentrations according to an IS92a emissions scenario. THC shutdown causes cooling of the Northern Hemisphere of $-1.7°C$, locally stronger. Over western Europe cooling is strong enough for a return to pre-industrial conditions and a significant increase in the occurrence of frost and snow cover. Global warming restricts the increase in sea ice cover after THC shutdown. This lessens the amount of cooling over NW Europe, but increases it over North America, compared to pre-industrial shutdown. This reflects a non-linearity in the local temperature response to THC shutdown. Precipitation change after THC shutdown is generally opposite to that caused by global warming, except in western and southern Europe, where summer drying is enhanced, and in Central America and southeast Asia, where precipitation is also further reduced. Local rise in sea level after THC shutdown can be large along Atlantic coasts (± 25 cm), which would add to the rise caused by global warming. Potentially rapid THC shutdown adds to the range of uncertainty of projected future climate change.

1 Introduction

Rapid, global-scale changes that are apparent in paleoclimate records of the last glacial cycle can be understood in terms of transitions between different ocean states (see Rahmstorf (2002) for a review). This interpretation is supported by several studies with more idealised numerical models, in which the ocean's thermohaline circulation ('THC')[1] has stable 'on' and 'off' states (Rahmstorf 1996; Gregory et al. 2003; Marsh et al. 2004). Elevated levels of atmospheric CO_2 (four times pre-industrial level) may cause a temporary, near-complete shut-down of

---

[1]In this paper we refer to the Atlantic meridional overturning circulation as 'thermohaline circulation'.

M. Vellinga (✉) · R. A. Wood
Met Office, Hadley Centre, FitzRoy Road, Exeter EX1 3PB, United Kingdom
e-mail: michael.vellinga@metoffice.gov.uk

the circulation (Stouffer and Manabe 2003). However, none of the more comprehensive general circulation models ('GCMs') used in the IPPC Third Assessment Report ('TAR') show a complete THC shutdown under a realistic forcing scenario for the 21st century. The consensus expressed in the TAR is that a complete collapse of the THC in the 21st century due to anthropogenic forcing of climate is less likely than discussed in the Second Assessment Report (Cubasch et al. 2001). Yet uncertainty remains in model formulation of GCMs, and hence model feedbacks that determine the THC response: even models that project a similar anthropogenic weakening of the THC do so for different reasons (Dixon et al. 1999; Mikolajewicz and Voss 2000). Rahmstorf and Ganapolski (1999) show that uncertainty in the (observationally poorly constrained) hydrological cycle can lead to uncertainty about the THC spinning down or not under anthropogenic climate change. Uncertainty in the change in tropical precipitation is particularly large (Murphy et al. 2004), which can have implications for the future of the THC (Latif et al. 2000; Vellinga and Wu 2004). Sytematic co-ordinated efforts are currently being undertaken to understand the spread in THC response to greenhouse gas forcing (Gregory et al. 2005). By applying observational constraints on model simulations the inter-model spread may be narrowed down within a given multi-model ensemble (Murphy et al. 2004; Schmittner et al. 2005), although the choice of relevant constraints is far from obvious. Furthermore, the full range of model uncertainty is difficult to sample completely. Based on the current evidence a full or partial THC collapse in the next 100 years can currently not be completely ruled out (Wood et al. 2003).

It is known from modelling studies that under pre-industrial climate conditions a large disruption of the THC would cool the Northern Hemisphere by several degrees (Manabe and Stouffer 1999; Vellinga and Wood 2002). If THC collapse were to occur in, say the year 2050, could it outweigh the effects of anthropogenic climate change, either locally or perhaps globally? More generally, how important are the effects of THC shutdown in the presence of global warming? It is also valuable to know to what extent climate behaves linearly: is the net effect of anthropogenic climate change and THC collapse simply the sum of the separate effects, relative to pre-industrial conditions? This is useful for risk assessment studies with integrated assessment models. In these class of models a priori assumptions are made about the physical climate response, rather than simulating these directly (such as the one used by McInerney and Keller (2007) elsewhere in this issue).

To address these questions we use the Met Office's Hadley Centre climate general circulation model HadCM3 (Gordon et al. 2000). Model and experiments are described in section 2. In section 3 we present a detailed analysis of the response in three important climate variables: temperature, precipitation and sea level. A summary and discussion are in section 4. In the present study we will focus on the climate response to THC collapse, which is strongest in the first few decades. An analysis of the feedbacks that control the long-term THC response will be discussed elsewhere.

2 Model and experiments

HadCM3 is a coupled, global ocean-atmosphere general circulation model. It is described in detail by Gordon et al. (2000), Pope et al. (2000), Cox et al. (1999), here we only give a brief summary. The atmosphere component has a horizontal resolution of $2.5° \times 3.75°$ and 19 vertical levels. The ocean component has a horizontal resolution of $1.25° \times 1.25°$ with 20 vertical levels, 10 of which are in the upper $300\,m$. The sea ice model uses a thermodynamic scheme, and ice is advected by surface currents. HadCM3 has a land surface scheme which

Fig. 1 CO_2 concentrations used in experiments G and PG (solid line). The dashed line is the constant pre-industrial CO_2 concentration used in C and P, 286 ppmv.
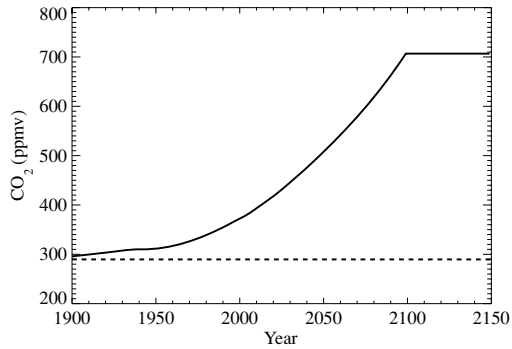
includes river run-off, and freezing and melting of soil moisture. The distribution of land ice is prescribed. Unless stated otherwise, decadally averaged model data are used here.

When greenhouse gas and aerosol concentrations are held fixed at levels typical of the late 19th century ('pre-industrial' era), the model's net radiative flux at the top of the atmosphere is close to zero. HadCM3 does not require flux adjustment to maintain a stable climate under these pre-industrial conditions. This model run is referred to as control, 'C', variables from this run will be indicated by subscripts 'c'. We also analysed an experiment in which HadCM3 is forced by increasing concentrations of CO_2 and other (minor) greenhouse gases. Between 1859–1990 historical greenhouse gas concentrations are used, between 1990-2100 concentrations rise according to an IS92a scenario. This experiment is referred to as greenhouse gas run, 'G', subscripted 'g'. It is described by Johns et al. (2003). We extended this experiment until 2160, with greenhouse gas concentrations held constant after the year 2100, Fig. 1. Wood et al. (1999) analysed the THC response to CO_2 increase in experiment G. They found that the THC weakened by about 20% over the course of the 21st century but did not collapse. This partial weakening can be understood in terms of changes to the ocean's heat and salt budget (Thorpe et al. 2001). Greenhouse gas forcing warms the ocean surface, which weakens the THC. Stabilising feedbacks that involve the hydrological cycle partially counteract this weakening, and limit the amount of THC weakening.

As argued in the Introduction, confidence in the accurate simulation of all processes that determine the strength of these feedbacks (and thus the overall THC change) is not absolute. We do need to understand the implications for climate of a potential THC collapse in the presence of anthropogenic climate change. Therefore, a THC shutdown was induced artificially by applying a large instantaneous freshwater perturbation to the North Atlantic between $50 - 90°$ N, equivalent to $5 \cdot 10^5$ km^3 of fresh water (this is 25 times the inferred North Atlantic freshening between 1965-1995 (Curry and Mauritzen 2005) all applied at once). This experiment will be referred to as 'PG'. It begins in 2049, and continues until the year 2160, with greenhouse gas concentrations evolving as in G. The perturbation is similar in design and magnitude to that of a previous experiment described by Vellinga et al. (2002) for pre-industrial conditions. We use results from that earlier experiment as well. It will be referred to here as experiment 'P', and nominally starts in 1849. Combining results from PG and P allows us to investigate if and how the climate response due to THC shutdown depends on the background climate state. We stress that the instantaneous freshwater perturbations in experiments P and PG were not intended to represent a plausible scenario, but only serve to force the model into a state with a weakened THC, from which the climate response can be calculated. All experiments are summarised in Table 1. A definition of anomalies and their use in this paper is presented in the Appendix.

**Table 1** Experiments used in this study

| Experiment	greenhouse gas forcing	freshwater perturbation
C	fixed late 19th century	-
P	fixed late 19th century	$5 \; 10^5 \; km^3$ instantaneous 1849
G	historical before 1990, IS92a from 1990–2100 then stabilised	-
PG	historical before 1990, IS92a from 1990–2100 then stabilised	$5 \; 10^5 \; km^3$ instantaneous 2049

3 Results

3.1 THC response

We use the maximum of the ocean's northward volume transport between 45–55° N in the Atlantic as a THC index. Using this index, the strength of the THC in C is just over 20 Sv, Fig. 2, in good agreement with observational estimates (Ganachaud and Wunsch 2000) ($1 \; Sv \equiv 10^6 m^3 s^{-1}$). As described by Wood et al. (1999), rising greenhouse gas concentrations in G lead to a gradual weakening of the THC from the late twentieth century. It is interesting to see that the THC weakening continues at a similar rate after the year 2100, when the greenhouse gas forcing remains constant. The weakening rate is about -0.3 Sv/decade between 2050–2100.

The overturning circulation in PG is substantially reduced within the first decade after the perturbation is applied, Fig. 2. It subsequently recovers at a rate of about 0.6 Sv/decade. The time evolution of P is also shown in Fig. 2. Not only is the strength of the THC in the first decade quite similar in P and PG, so are their spatial structures (not shown here, but that of P is shown Fig. 3b of Vellinga et al. (2002)). Furthermore, experiment PG shares with P the tendency of the THC to recover from the collapsed state. This collapsed state is not stable under pre-industrial conditions, nor with raised greenhouse gas concentrations. However, the
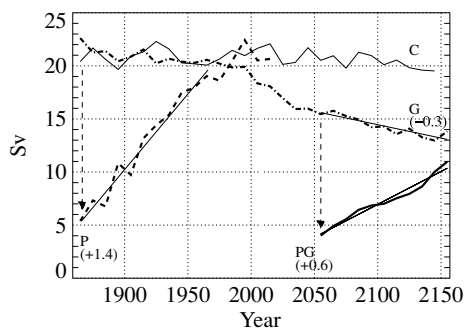
Fig. 2 Time series of THC strength (defined as the maximum meridional stream function in the Atlantic between 45–55° N). The curve labelled 'C' (thin solid) is from the control run; the curve labelled 'P' (dashed) is from the run where the freshwater perturbation was applied in 1849 (indicated by arrow), using thse same fixed pre-industrial greenhouse concentrations as C. The curve labelled 'G' (dash-dot) is from the run with varying greenhouse gas concentrations (see text for details), 'PG' (heavy solid) from the run using the same time-varying greenhouse gas concentrations, but with a freshwater perturbation applied in 2049 (indicated by arrow). The numbers in brackets are the rate-of-change of the THC strength in *Sv/decade* in each experiment, calculated as the linear trend over the period indicated by the thin straight lines.

Fig. 3 Surface air temperature over Northern Hemisphere land, labels indicate the experiments. Crosses are the estimated linear response.
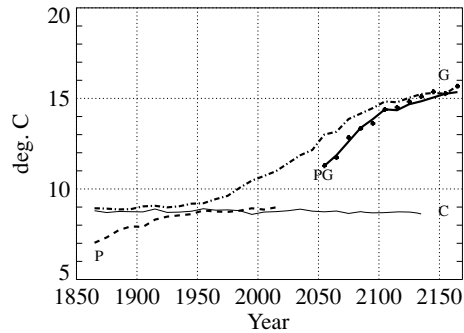
recovery occurs at a rate that is more than twice as slow: +0.6 Sv/decade, compared to 1.4 Sv/decade for P.

The THC recovery rate in PG is not simply that of P minus the anthropogenic weakening rate from G. Clearly, the feedbacks that set the recovery rate of the overturning in HadCM3 depend non-linearly on the background climate, and therefore depend on the evolution of greenhouse gas concentrations after the year 2100. To understand the processes that set the recovery time scale in HadCM3 is not the aim of the present paper, and will be discussed elsewhere.

3.2 Global temperature response

THC shutdown in experiment PG is initiated against a background of global warming, which is caused by rising greenhouse gas concentrations according to an IS92a scenario. Relative to this global warming the THC shutdown causes cooling of surface air temperature ('SAT') over the Northern Hemisphere (Fig. 3), and slight warming over the Southern Hemisphere (not shown). Cooling is $-1.7°$C during the first ten years. In subsequent years recovery of the THC accelerates the rate of warming, and SAT catches up with that of greenhouse gas run G by the year 2150. Temperatures from the control run, and pre-industrial perturbation P are also shown. The change in Northern Hemisphere temperature after THC shutdown is similar in P and PG. This is reflected in the good estimate given by the linear response (shown by the crosses in Fig. 3: adding SAT anomalies from pre-industrial shutdown to SAT of experiment G provides a good approximation of the actual response in PG.

The pattern of SAT anomaly during the first 10 years is shown in Fig. 4. The area on the Northern Hemisphere where cooling due to THC shutdown outweighs the warming due to anthropogenic greenhouse gas increase, and lowers temperature below pre-industrial levels is outlined by the heavy black line. This region covers most of the North Atlantic, and the westernmost fringes of Europe.

This pattern of temperature response largely resembles that of the change 20–30 years after THC shutdown under pre-industrial conditions (experiment P) from Vellinga and Wood (2002). There are differences, however. Some of these (e.g. the weaker Southern Hemisphere response in Fig. 4) arise because there has not been enough time for them to be established after just 10 years. (Strictly speaking, Fig. 4 should therefore be compared to the change in years 0-10 in experiment P. For brevity it is not reproduced here, but is shown as Fig. 1a of Wood et al. (2003)). Other changes in SAT are more fundamental, and reflect a non-linearity in the THC-driven response. Figure 5 shows this nonlinearity: it is the difference between the response due to the THC shut-down in 2049 and in pre-industrial during the first ten years
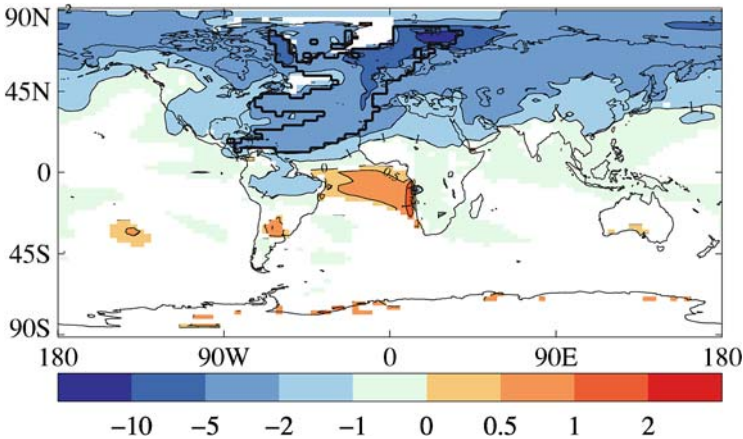
Fig. 4 Difference in surface air temperature between experiments PG and G in the years 2049–2059. This difference is therefore the temperature change that a sudden THC shutdown would cause relative to an IS92a global warming scenario in 2049–2059. The area where cooling causes temperature to fall below pre-industrial conditions is outlined by the heavy solid line, areas where the difference is not significant have been masked.

($\Delta\mathrm{SAT}_{\psi g} - \Delta\mathrm{SAT}_{\psi c}$ using the terminology of the Appendix). THC collapse in 2049 causes less cooling than in pre-industrial times over the Greenland-Norwegian Seas, Northwestern Europe, Greenland and most of the Arctic, stronger cooling over much of North America, and stronger warming over Antarctica.

The nonlinearity in the (sub-) Arctic is due to a different sea-ice response. Because of the ice-albedo feedback (more sea ice increases the amount of solar radiation that is reflected, lowering temperature), and of the insulating effect of sea ice on the air-sea heat flux, there is a strong control of sea ice cover over air temperature in this region. After THC shutdown, the northward ocean heat transport across $60°$ N is reduced by about 0.2 PW in both experiments
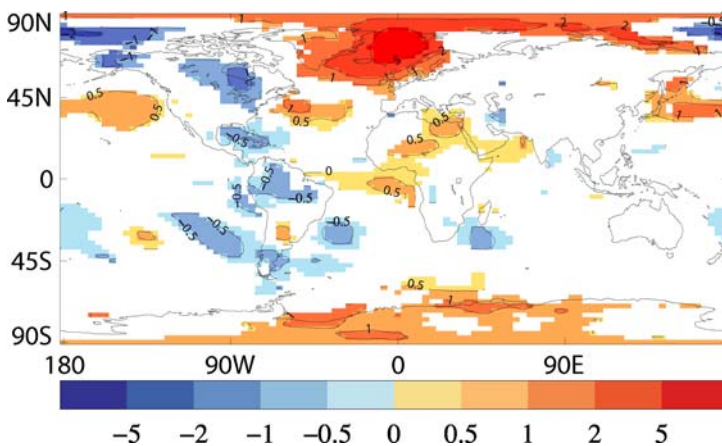
Fig. 5 Difference in temperature change after THC collapse in 2049 (PG-G) minus that under pre-industrial conditions (P-C), i.e. $\Delta\mathrm{SAT}_{\psi g} - \Delta\mathrm{SAT}_{\psi c}$. Regions where the nonlinearity lies within the noise level of internal variability have been masked.

Fig. 6 Sea-ice cover in the Greenland-Norwegian Sea (between 20° W–20° E and 60° –80° N)
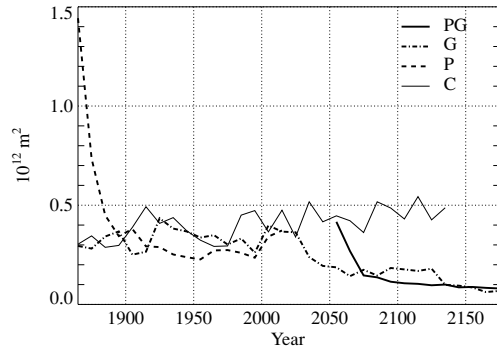
PG and P. The subsequent fall in temperature of the upper $100\,m$ of the Greenland-Norwegian Seas is also very similar, $5°\,C$ in both cases. In pre-industrial experiment P this cooling leads to a sharp increase in sea-ice cover in the first decade (Fig. 6, see also Fig. 6 of Vellinga et al. (2002)). Because of global warming the surface layers of the Greenland-Norwegian Seas have warmed by nearly $2°\,C$ by the year 2049 . The THC collapse induced in PG in 2049 therefore leads to a smaller volume of the Greenland-Norwegian Seas to cool to freezing level. The increase in sea ice cover is only 20% of that after pre-industrial THC collapse, Fig. 6, and the average cooling of surface air temperature in the region is reduced by $5°\,C$, Fig. 5. The same happens to a lesser degree in the Sea of Okhotsk, which causes the reduced cooling over the North Pacific.

The changes in sea level pressure in PG are such that more cold air flows from the Arctic into North America than happens in P (not shown). This explains the enhanced cooling by up to $1°\,C$ in North America, Fig. 5. Circulation changes in the atmosphere cause a different SAT response further south, in the tropics and over Antarctica. Over Antarctica warming after THC shutdown in 2049 is about an extra degree, compared to shutdown in the pre-industrial era. This would have implications for the Antarctic ice sheet, and hence global sea-level, which we will explore in section 3.5

Even though Northern Hemisphere mean SAT change over land after THC shutdown in a pre-industrial climate and a 21st century climate are similar in magnitude, there are important regional differences.

3.3 Regional temperature change

Because the seasonal cycle varies between climate zones, it is not clear a priori if and how THC shutdown affects seasonality in different parts of the world. In Fig. 7(a–d) we show seasonal temperature cycles in four regions: western Europe, eastern North America, south Asia and Central America. We show the mean annual cycle as simulated by HadCM3 under pre-industrial conditions (C), with greenhouse gas forcing between years 2050–2060 (G) and with greenhouse gas forcing and THC shutdown in the same period (PG). To assess the linearity in the temperature change in PG, we also show by crosses the superposition of temperature from the greenhouse gas experiment (G) and anomalies following THC shutdown in pre-industrial (P-C). Differences between the crosses and solid curve that exceed the amount of internal variability indicate a non-linear temperature response.

In western Europe increased greenhouse gas concentrations lead to a marked warming by 2050 (G), compared to pre-industrial conditions (C). The warming is strongest in summer. This greenhouse gas warming means that when THC shutdown is initiated in 2049 (PG),
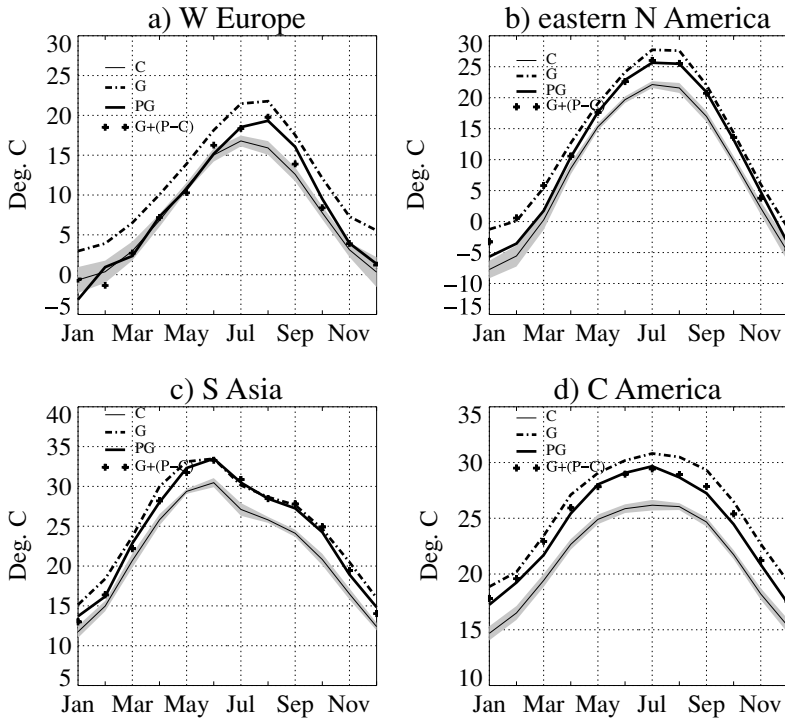
Fig. 7 Average annual cycle of surface air temperature over land in: (a) western Europe (20° W–15° E; 45–55° N) (b) eastern North America (100–50° W; 30–50° N) (c) south Asia (60–90° E; 0–30° N) (d) central America (115–50° W; 10–30° N). The annual cycles were calculated using monthly mean values from years 2050–2060 for PG (heavy solid) and G (dash-dot). For C (thin solid) we used 300 years of data, the grey shading indicates for each month the range of two decadal standard deviations. Crosses indicate the temperature from experiment G to which the anomaly from pre-industrial THC shutdown (P-C) has been added, i.e. the linear response.

climate cools, but not to the extremely cold conditions that would follow THC shutdown in pre-industrial. In fact, the anthropogenic warming in summer is so large that even after THC shutdown in 2049 (PG) temperature between June and September remains above pre-industrial conditions. From October to May mean temperature cools to levels within the range of variability under pre-industrial conditions. Temperature response in PG is essentially linear, except in September and October, when the fall in temperature is less than that based on a linear superposition.

In eastern North America the THC shutdown in 2049 also causes cooling. Between November and April cooling is particularly strong, and temperature returns to near or just above pre-industrial values. In fact, temperatures between January and March are colder than a linear superposition would suggest. As discussed in the previous section, this is linked to the different response in the circulation over the Arctic. Between May and November cooling is weaker than in the rest of the year, and temperature remains well above pre-industrial levels. In south Asia the THC disruption leads to cooling between October and May. This is during the Northeast monsoon, when the circulation brings in air from the north, that is cooled by THC shutdown. During the Southwest monsoon there is no significant cooling. Temperature response is linear year-round. THC disruption in 2049 does not lead to a return
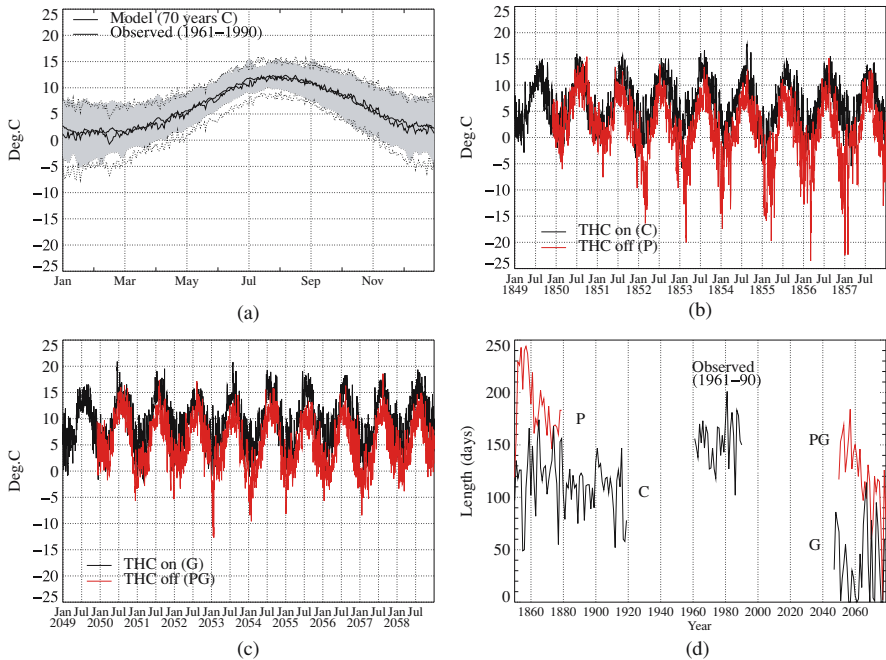
Fig. 8 (a) Annual cycle of daily minimum Central England Temperature ('CET') as observed in the period 1961–1990 (thin solid for average minimum, dotted for the 5th/95th percentiles), and averaged over 70 years of the control experiment C of HadCM3 (heavy solid for the average, grey shading for the range of 5th/95th percentiles. (b) Simulated daily minimum CET for control experiment (C, black), and first 10 years after THC shutdown in pre-industrial (P, red). (c) As in (b), but for greenhouse gas experiment G (black), and first 10 years after THC shutdown in 2049 (PG, red). (d) Length of frost season. We used 30 years of daily values for P, G and PG, and 70 years for C. For the observed period we used daily values for the period 1961–90.

to pre-industrial temperature at any time. In Central America, THC shutdown cools climate uniformly throughout the year, in a linear way.

We conclude this section with an analysis of simulated changes in daily Central England Temperature ('CET'). Because the observed record of daily CET goes back to 1772 (Parker et al. 1992) this is a useful way to put the effects of THC shutdown on climate of the UK in perspective. Comparison with the observed record for the period 1961–90 shows that HadCM3 has useful skill in simulating mean as well as extreme CET throughout the year (Fig. 8a). We therefore have some confidence in using this global model to estimate changes in mean and extreme values of CET after THC shutdown under pre-industrial conditions in 1849 (Fig. 8b), and 2049 (Fig. 8c). For the first year of either experiment there is no apparent cooling over the UK. From the second year after THC shutdown minimum CET is consistently colder than in the respective unperturbed experiments (C and G). Winters in pre-industrial experiment P become increasingly cold from the third winter (1851/52). In addition to spells when winter temperatures are near-normal, there are also prolonged periods when minimum temperature falls below the 5th-percentile of the control, $-3.3°$ C. This happens for about 40% of the time in the winters between 1850-1860. During these cold spells average minimum temperature is $-8°$ C, the coldest minimum temperature is $-22°$ C. These cold periods are associated with northerly winds that bring air from an ice-covered Norwegian Sea to the UK. Temperatures after THC shutdown in 2049 also take

Table 2 Average Central England Temperature in $^\circ$C during winter months (DJF), and standard deviation of 30-year-mean temperature for control. Listed are average daily minimum (T_{min}), average daily maximum (T_{max}) and average daily mean (T_{mean}) values. Years over which the averages are calculated are shown in brackets, 'obs' refers to observed CET data

Source	T_{min}	T_{max}	T_{mean}
PG (2049–59)	1.1	5.7	3.0
G (2049–59)	5.1	9.4	7.3
P (1849–1859)	−3.1	1.2	−0.9
C	2.0 ± 0.1	6.1 ± 0.1	4.1 ± 0.1
obs (1961–90)	1.4	6.7	4.1
obs (1962/63)	−3.1	2.5	−0.3
obs (1979/80)	−1.1	4.3	1.6

about a year to fall below 'normal', i.e. those of greenhouse gas experiment G. There are spells when temperature in PG also falls below -3.3°C, but these occasions are less frequent (10% of the time) and not as cold as in P (-5.8°C on average, with coldest temperature of -12°C). Less cold mean and extreme minimum temperature are consistent with elevated CO_2 levels, and the smaller increase in sea-ice cover over the Norwegian Sea after THC shutdown.

In Table 2 we list the average CET for the entire winter during the first ten years of the various model runs. For illustrative purposes we also list observed values, including those of the winter of 1962/63 (the coldest winter in the CET series), and 1979/80 (the coldest most recent winter). The winter of 1962/63 is a good analogue for the average winter during the first ten years of experiment P. On average, winter mean CET in the first ten years after THC shutdown in 2049 would be colder than the observed average for the period 1961–90 (3°C vs. 4.1°C). In fact, only five winters in the period 1961–90 had a mean temperature colder than 3°C. Severity of a particular winter is not just defined by temperature, but also by the duration of the cold period. We calculated the length of the frost season, here defined as the number of days between the first frost in autumn, and the last frost in the following spring, based on daily minimum CET. This quantity would be relevant to agriculture. Because the model has a warm bias of the 5th percentile CET for much of the year in control experiment C (Fig. 8a), simulated length of the frost season is too short (on average 111 days), compared to the equivalent based on observed CET (150 days), Fig. 8d. In the first ten years of P, the frost season almost doubles in length, reducing the frost-free period from about eight months to five months per year. In the first ten years after THC shutdown in 2049 the frost season more than triples in length (147 days in PG, compared to just 41 in G). In experiment G years without any frost at all are quite common by then (21% of the time), whereas frost-free years do not occur after THC shutdown in PG. THC shutdown in 2049 would make winters considerably more severe compared to pre-industrial.

3.4 Precipitation and snow cover

The change in precipitation after THC shutdown is significant over much of the Northern Hemisphere, and the tropics, Fig. 9a. Consistent with cooler conditions, when air can hold less water vapour, most of the Northern Hemisphere receives less precipitation. The response is particularly strong over the tropical Atlantic, where rainfall decreases north of the equator, and increases south of the equator. This is indicative of a southward shift in the ITCZ over the
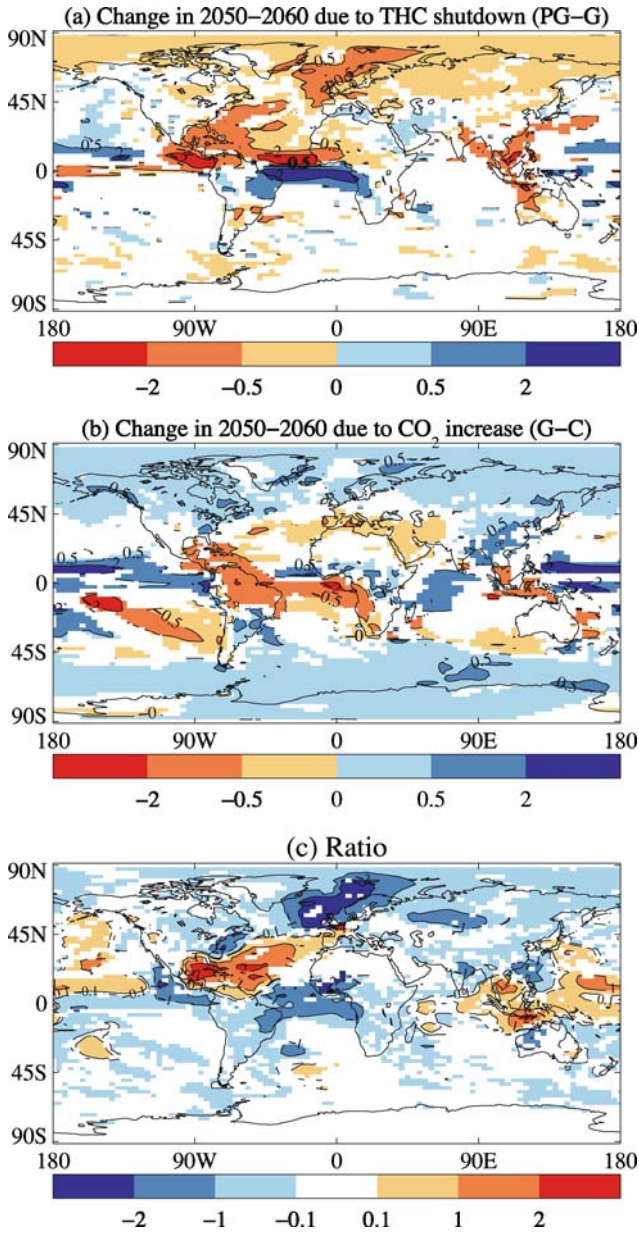
Fig. 9 Change in precipitation (in mm/day) in 2050–2060 (a) due to THC shutdown (experiment PG minus experiment G) (b) due to increased GHG concentrations (experiment G minus control). Points where the changes are not significant have been masked. (c) THC-induced change (data of Fig. a) divided by GHG-induced change (data of Fig. b). Grid points with small changes in the latter would cause singularities and are masked. A 5x5-point smoother was applied to highlight large-scale features.

Atlantic. At the large scale the response is similar to that after pre-industrial THC shutdown (Vellinga and Wood 2002). There are differences, however, but unlike the temperature response, these 'non-linearities' have a complex spatial structure and are not discussed here. It is more informative to quantify how the response to THC shutdown compares to the change in precipitation due to increase greenhouse gas concentrations.

As described by Johns et al. (2003), and shown here in Fig. 9b, under increased greenhouse gas concentrations HadCM3 projects stronger precipitation at high latitudes, and a reduction in the subtropics. This is indicative of a more vigorous hydrological cycle (Allen and Ingram 2002). The response in the tropics has a complex structure, including northward shift in the ITCZ over the Atlantic, and drying over much of northern South America. In general, the precipitation response to increased greenhouse gas forcing is in the opposite sense to that after THC shutdown. This is presumably because the temperature response is opposite in both cases: the Northern Hemisphere warms due to climate change, but cools due to THC shutdown. To quantify the relative importance of either effect, we calculated the ratio of the THC response and the greenhouse gas response, Fig. 9c. Where this ratio is positive THC response reinforces the greenhouse gas response, where it is negative, THC-shutdown counteracts the greenhouse gas response. The strongest effect, in relative terms, occurs over the Atlantic region. At high latitudes the THC-related drying more than compensates for the greenhouse gas-related precipitation increase. Near the equator, as seen before, the effects on the ITCZ and changes in precipitation also are opposite and of equal strength. Over the subtropical North Atlantic the THC shutdown reduces rainfall, reinforcing the reduction in rainfall occurring under global warming. This affects adjacent land masses of Central and northern South America, and southwest Europe. Over much of Asia the THC shutdown causes a reduction in rainfall. This adds to the drying over Southeast Asia caused by greenhouse gas increase, and cancels out the increase in rainfall over India. Examples of annual cycles of precipitation with and without THC shutdown are given in Fig. 10. Over northwestern and southern Europe, the THC shutdown exacerbates summer drying under increased greenhouse gas concentrations. This is consistent with the notion that a larger land-sea temperature contrast (to which THC shutdown would add, Fig. 4) is important in causing expected summer drying (Rowell and Jones 2006). Over northwest Europe, the THC shutdown cancels the enhanced winter precipitation due to global warming. Rainfall associated with the Indian southwest monsoon is reduced. Over Central America rainfall is also further reduced. The linear response generally provides a reasonable approximation of the sign, if not magnitude, of precipitation change after THC shutdown.

In a colder climate, we expect more of the precipitation to fall in the form of snow. Also, at lower temperatures, any snow cover is likely to last longer. A global climate model like HadCM3 can only marginally resolve details of orography, and land surface, and a regional model with higher resolution would be more suitable (Jacob et al. 2005). Nevertheless, the results presented here will provide some indication of the changes in snow cover that THC shutdown in the 2050s could cause. The snow cover in the period 2050–60 with and without THC shutdown is shown in Fig. 11. Using daily values, we calculated the maximum snow depth in the winter months (here taken between November–April) in experiments PG and G. Without THC shutdown, western Europe is unlikely to have any snow cover by the 2050s; after THC shutdown, maximum snow depth between 1–5 cm, however briefly, would be the norm. Maximum snow depth would also increase over central and eastern Europe, and Scandinavia. The period in winter with at least 3 cm of snow cover would increase accordingly: from virtually no occurrences in the 2050s without THC shutdown, to up to 10% of the time over western Europe after THC shutdown.
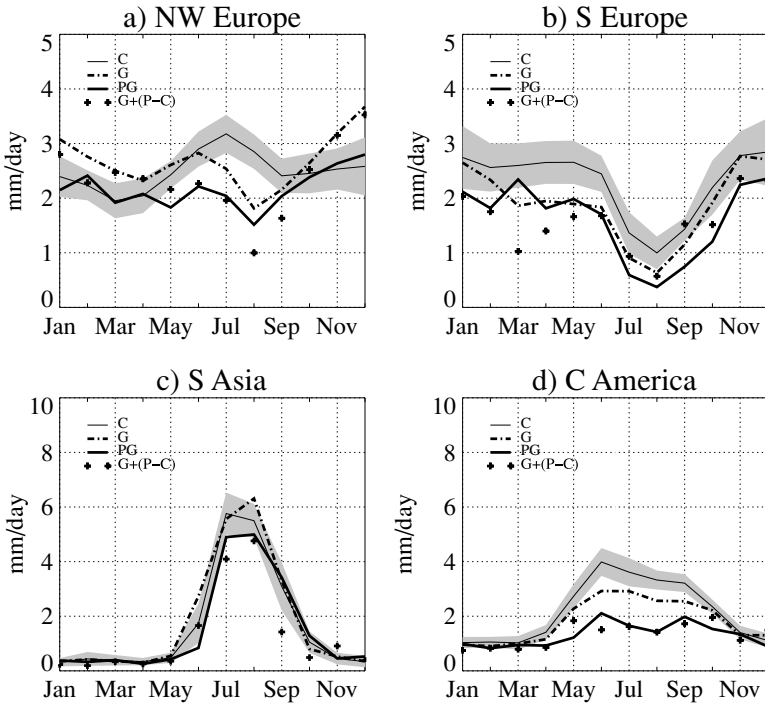
Fig. 10 Average annual cycle of total precipitation (in mm/day) over land in: (a) northwest Europe (20° W–15° E; 50–70° N) (b) southern Europe (10° W–30° E; 35–45° N) (c) south Asia (60–90° E; 0–30° N) (d) central America (115–50° W; 10–30° N). The annual cycles were calculated using monthly mean values from years 2050–2060 for PG (heavy solid) and G (dash-dot). For C (thin solid) we used 300 years of data, the grey shading indicates for each month the range of two decadal standard deviations. Crosses indicate the precipitation from experiment G to which the anomaly from pre-industrial THC shutdown (P-C) has been added, i.e. the linear response.

3.5 Sea level

Sea-level height can change in response to several factors. Firstly, if the density of the ocean changes (for instance due to global warming), the water column will expand or contract, leading to a change in global sea level. This may be modified by changes in the THC (Knutti and Stocker 2000). Secondly, if water stored on land is transferred into the ocean (e.g. due to melt of glaciers, or continental ice sheets) this will create a rise in global sea level. In addition to global sea level change, change in ocean currents (e.g. associated with changes in the THC) causes local changes to sea level, which we will refer to as dynamical sea level change. Gregory (1993) gives a detailed discussion of the processes determining sea-level change. In a recent study Levermann et al. (2005) use a climate model to quantify the change in sea level associated with a weakening of the THC. Because the deep ocean gradually warms in response to THC slowdown, thermal expansion causes global sea level rise, which Levermann et al. (2005) find to be of the order of 10 cm over a 200 year period. Along North Atlantic coasts they report a more rapid dynamical sea-level rise of up to 50 cm, due to a weakening of the North Atlantic Current.
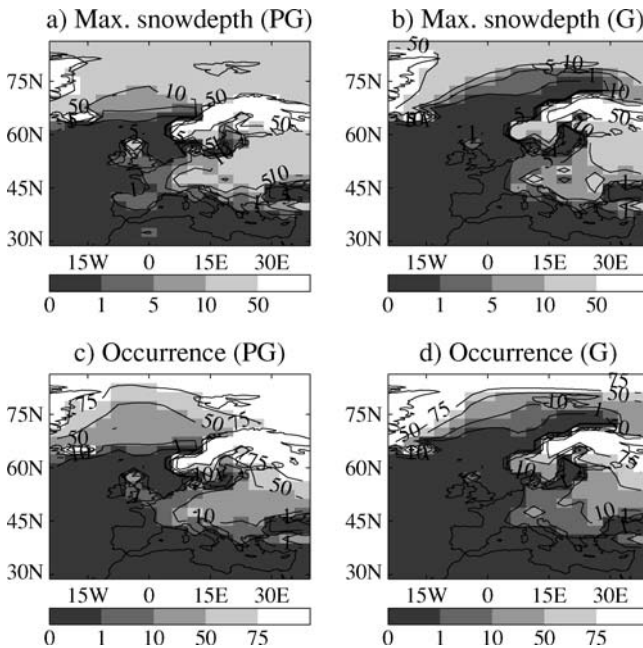
Fig. 11 (a) Maximum snow depth (in cm), averaged over the ten winter seasons (November–April) between 2050–60 of experiment PG. (b) As in (a), but for experiment G. (c) Occurrence (as a percentage of the time) of a snowdepth of at least 3 cm, averaged over the ten winter seasons between 2050–60 of experiment PG. (d) As in (c) but for experiment G.

As pointed out in section 2, the large instantaneous freshwater perturbation used in experiments P and PG was not intended to represent a plausible scenario. It should be kept in mind that aspects of sea-level change depend on the transient model state in these experiments (e.g. the duration of the THC weakening, and the nature of the change in ocean currents, which will depend on where the freshwater perturbation is applied). Results presented here should be considered as an order of magnitude estimate of sea level rise due to THC shutdown, in the presence of global warming. Our methods for calculating sea-level height are summarised in the Appendix. Anthropogenic sea level change in experiment G (i.e. without THC shutdown) until the year 2100 has been described by Gregory and Lowe (2000).

Anthropogenic forcing of climate in experiment G causes the ocean's interior to warm, and thermal expansion leads to a gradual sea level rise (Fig. 12a, see also Gregory and Lowe (2000)). Between 1859–2049 global sea level rises by about 15 cm. Slow-down of the THC in 2049 leads to additional warming of the ocean, giving an extra sea level rise of about 1–2 cm between 2049–2100. This extra expansion due to THC is of similar magnitude as that of experiment P for pre-industrial THC shutdown. In our experiments P and PG, the recovery of the THC reverses the ocean warming, which prevents the thermal expansion from reaching the large values associated with permanent THC shutdown (Levermann et al. 2005).

The cooling of the Northern Hemisphere following THC shutdown increases accumulation of snow over the Greenland ice sheet and the smaller glaciers. The warming of the Southern Hemisphere also leads to a growth in the Antarctic ice sheet volume, because of more precipitation. In pre-industrial climate this increase in land-ice volume lowers sea-level by an estimated 12 cm, Fig. 12b. Between 2049–2150 THC-shutdown also reduces sea-level
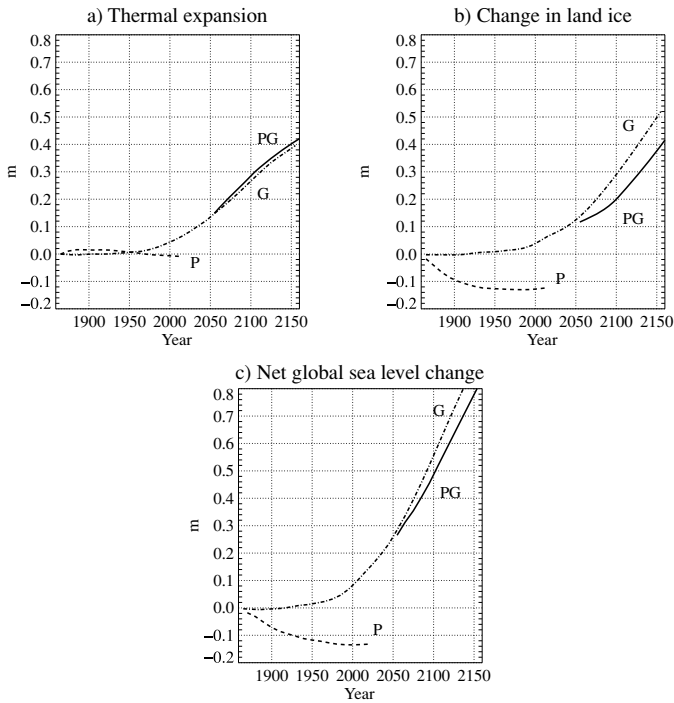
Fig. 12 Global sea-level change due to (a) thermal expansion (b) change in land-ice volume (c) net change, i.e. sum of (a) and (b).

rise by up to 12 cm. The effect of change in land ice volume on global sea level is thus quite similar between P and PG, in spite of the difference in temperature change at high northern and southern latitudes (Fig. 5). The weaker cooling over the Northern Hemisphere in 2049 is offset by the enhanced warming over Antarctica. The effect of THC shutdown on thermal expansion and land ice act in an opposite sense. The effects of THC shutdown on a change in land-ice dominate those of thermal expansion, and the global sea level rise due to increased greenhouse gas concentrations is reduced by up to 10 cm between 2049–2150 (Fig. 12c).

The net change in regional sea level also has a dynamic component. For years 2050–2060 we calculated the net change in sea level, i.e. the sum of change in dynamical sea level height (which has a local effect, but no contribution to global mean sea level change) and global mean sea-level change (due to thermal expansion and change in land ice). For greenhouse gas forcing alone (experiment G, Fig. 13a), the net change is fairly uniform across the oceans, i.e. it shows mainly the global mean rise. There is some regional variation in the Arctic and Southern Ocean. The major re-organisation of the circulation in the North Atlantic Ocean after THC shutdown in 2049 (PG) leads to large regional variations in sea level change, Fig. 13b. In the open ocean changes occur in excess of 1 m. Along the Atlantic coasts of Europe and North America changes are 25–50 cm. If we remove the sea level change due to global warming (PG-G, Fig. 13c) we get the pattern associated with THC shutdown (cf. Equation 4, Appendix). This THC-related sea level rise in the North Atlantic is 'fed' by a largely uniform lowering of sea level everywhere else, except the North Pacific. In the northern North Atlantic sea level rise in Fig. 13c is comparable to that of Levermann et al. (2005). The drop in sea level south of about 40° N, however, is in contrast with the overall

Fig. 13 Net sea level change relative to pre-industrial climate. This is the sum of change in dynamical sea level (which has no contribution to global mean sea level) and a change in global mean sea level (due to thermal expansion and melting of land ice). a): Sea level rise averaged over the period 2049–59 caused by greenhouse gas increase alone, experiment G b): Change in 2049–59 caused by greenhouse gas increase and THC shutdown, experiment PG c): Change in sea level caused by THC collapse in 2049, i.e. the difference between PG and G. Values are in m, with contours at ±0.05, ±0.25, ±0.5 and ±1m, zero contour is heavy, negative contours are dashed. Regions where sea level rises by more than 0.5m are hatched, regions where it falls are stippled.
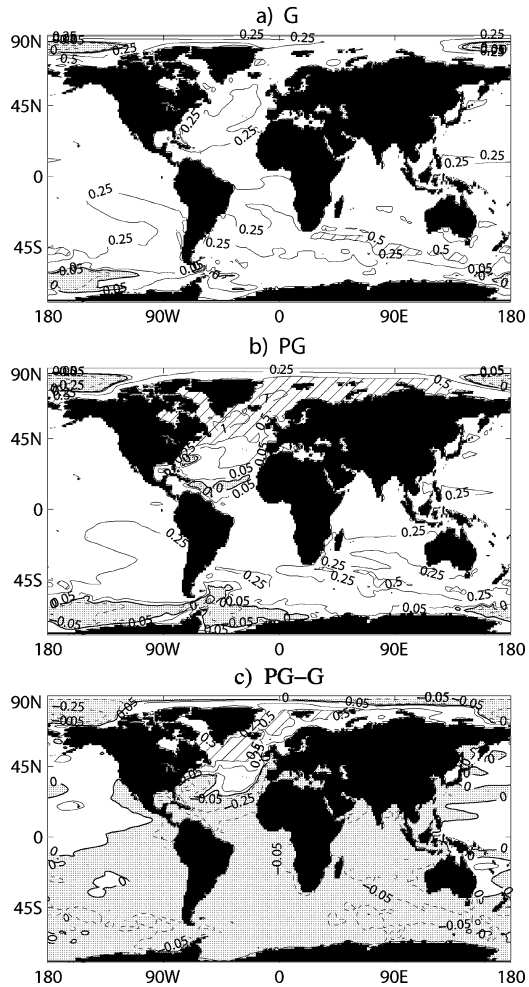
rise in dynamical height in the Atlantic of Levermann et al. (2005). This indicates that details of local sea-level change due to THC shutdown depend on the time-history (magnitude, rate and timing) of the changes in the ocean circulation and winds, and probably model formulation. This makes the change difficult to project, not unlike the regional sea level change caused by global warming (Church et al. 2001). Importantly, both the analysis by Levermann et al. (2005) and the present study clearly indicate the possibility of large regional sea level changes following THC shutdown, that could add to the sea level rise caused by global warming.

4 Discussion and conclusions

To determine the effects of a potential THC shutdown ('rapid climate change') on climate of the mid-21st century, when greenhouse gas concentrations in the atmosphere have increased well above present-day levels ('global warming'), we carried out a sensitivity experiment

with the global climate model HadCM3. With greenhouse gas concentrations increasing according to an IS92a scenario, we apply a large instantaneous fresh anomaly in the North Atlantic in the year 2049. The THC in the model all but shuts down within a few years after the perturbation is applied. It then gradually recovers in about 100 years to near the strength it has in the unperturbed case. This indicates that this state of the model without THC is not stable. We use this idealized approach because under realistic scenarios the model does not show a shutdown of the THC. Nevertheless, the confidence in the model's ability to correctly simulate all positive and negative feedbacks accurately is not complete. A large, possibly complete, THC shutdown in the 21st century cannot be ruled out.

After THC shutdown, the Northern Hemisphere land areas cool (on average by -1.7° C). This is similar to the cooling after a pre-industrial THC shutdown. Strongest cooling occurs in western Europe and Scandinavia (by 2–5° C). Along the western fringes of Europe cooling is strong enough for temperature to fall below pre-industrial levels. Elsewhere, temperature remains above pre-industrial values. Downscaling experiments with a high-resolution regional model suggest that cooling may penetrate further into continental Europe than suggested by our global model (Jacob et al. 2005). The amount of cooling over western Europe depends somewhat on the timing of our experiment, because of a sea-ice feedback. If THC shutdown had been induced earlier, cooling over Europe would be stronger, because of a larger increase in sea ice cover. At regional scale this introduces a nonlinearity in the temperature response, because its magnitude depends on the state of the background climate. We have quantified some effects of THC shutdown on winters in the UK. This region would experience winter temperatures considerably colder than those typical of 1961–90, and a threefold increase of the period during which frost occurs in a year.

Precipitation after THC shutdown is reduced over much of the Northern Hemisphere, over land by on average 6 cm/year. Precipitation changes are generally in the opposite sense to those caused by rising greenhouse gas concentrations. However, THC shutdown exacerbates summer drying in western and southern Europe caused by increased greenhouse gas levels. Furthermore, in Central America and southeast Asia THC shutdown reinforces the reduction of precipitation. Local change in sea level after THC shutdown can be fast and large, 25–50 cm along the north Atlantic coast lines. The pattern of sea level change depends on the transient ocean circulation change, which is rather difficult to predict. Changes in precipitation and sea level are potentially large and can affect regions beyond the North Atlantic. Therefore, impact studies of THC shutdown in which these effects are ignored, and only temperature change is considered, will miss important aspects of the global climate response.

Generally speaking, THC shutdown changes the sign of the climate change caused by global warming. But there are instances where THC shutdown causes changes that work in the same direction, reinforcing those caused by global warming (e.g. regional change in sea level and precipitation). It has been suggested that sign reversal could pose challenges for society to adapt to (Hulme 2003), presumably more so for more rapid transitions. Furthermore, the possibility of a sign reversal implies that there is a wider range of possible futures that need to be taken into account when considering adaptation to climate change. We illustrate this point using late-winter sea ice distribution as an example, Fig. 14. Rising greenhouse gas concentrations ('G', red lines) lead to a northward withdrawal of sea ice by the 2050s, compared to the pre-industrial case (shading). Most of the Norwegian Sea and the western Barentsz Sea will be ice-free in late winter under this forcing scenario. By contrast, if the THC should collapse in 2049 with greenhouse gas concentrations according to an IS92a scenario ('PG', white solid lines), our experiments suggest that sea ice would return to the area, and extend further southward than at present-day. The nearer in the future THC shutdown occurs, the more closely sea ice cover would resemble that of the pre-industrial case ('P', white
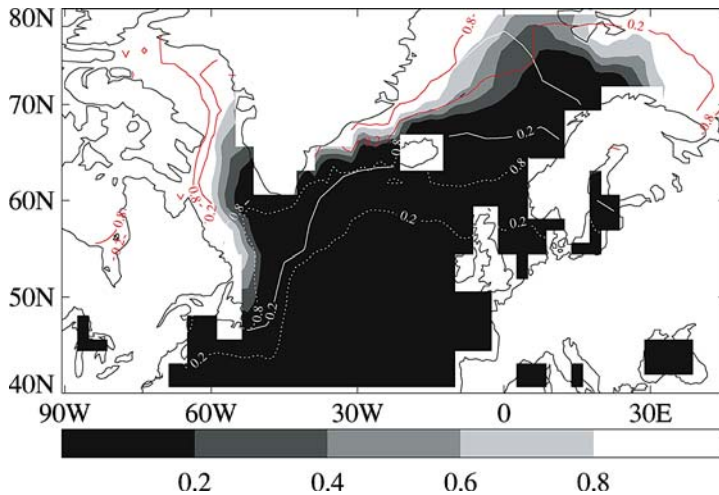
Fig. 14 Sea ice distributions in March. The grey shading shows the model's distribution under control (pre-industrial) conditions. Positions of 20% and 80% sea ice cover isolines are shown for the case of global warming under an IS92a scenario (red, years 2055-60, 'G'), combination of global warming and THC shutdown (white solid, years 2055-60, 'PG'), years 5-11 after pre-industrial THC shutdown (white dotted, 'P'). These three cases are substantially different in terms of regions free of sea ice cover, and would probably suggest different adaptation strategies for the region.

dotted lines), for which the 20% cover reaches the British Isles and New England. When deciding on adaptation strategies to climate change, these three cases would imply different choices. In all of this one needs to take into account the small (Cubasch et al. 2001), but as yet unquantified likelihood of rapid THC shutdown ('PG' or 'P') compared to that of gradual weakening under a climate change scenario ('G').

To provide an objective risk assessment of THC shutdown is a challenge posed to the scientific community. Firstly we need to understand the reasons why the models' THC responds differently to greenhouse gas forcing (Gregory et al. 2005), and test this model-based understanding against observations where possible. Observations are unlikely to completely constrain models, and we need a concerted effort to quantify this model uncertainty (e.g. Murphy et al. (2004); Stainforth et al. (2005)), and then consider how this knowledge can be translated into a meaningful THC risk assessment strategy (Wood et al. 2006).

Appendix

Defining anomalies

If climate is perturbed, either through anthropogenic forcing (subscript 'g'), or the combined effects of THC disruption and anthropogenic forcing ('pg'), a climate variable (indicated here as 'Φ') will undergo a change compared to pre-industrial, or control, conditions ('c'):

$$\Delta \Phi|_{pg} = \Phi|_{pg} - \Phi|_{c} \qquad (1)$$

$$\Delta \Phi|_{g} = \Phi|_{g} - \Phi|_{c} \qquad (2)$$

If $\Delta \Phi|_{pg}$ is written as the sum of anthropogenic forcing and a contribution of the THC disruption at elevated CO_2 levels '(ψg)':

$$\Delta \Phi|_{pg} \equiv \Delta \Phi|_g + \Delta \Phi|_{\psi g} \tag{3}$$

re-arranging terms gives for $\Delta \Phi|_{\psi g}$:

$$\Delta \Phi|_{\psi g} = \Phi|_{pg} - \Phi|_g \tag{4}$$

For change in Φ after THC disruption under pre-industrial conditions '(ψc)' we have:

$$\Delta \Phi|_{\psi c} = \Phi|_p - \Phi|_c \tag{5}$$

A difference between $\Delta \Phi|_{\psi g}$ and $\Delta \Phi|_{\psi c}$ indicates a non-linearity in the climate response due to THC disruption, because it means that the response depends on the 'background' climate state at which the THC disruption occurs (i.e. pre-industrial climate, or climate altered by elevated atmospheric greenhouse gas concentrations).

Sea level change in HadCM3

HadCM3 is a rigid-lid model, so sea surface height is not a prognostic variable. The model conserves volume, and not mass, which is what happens in the real ocean. Nevertheless, the various contributions to sea level rise can be calculated off-line, as described in detail by Gregory (1993), and summarised here. The sea level change due to thermal expansion is calculated by assuming that the change in density leads to a local expansion in each model grid box. Subject to the constraint that the mass in each grid box does not change during this expansion we can estimate the change in volume, and hence sea level rise. The effect of salinity change on density is ignored in the calculations of expansion, and we use constant long-term model mean salinity instead. A small drift of global average salinity in the control experiment necessitates this (Gregory 1993; Gregory and Lowe 2000). More importantly, the very strong salinity perturbation that we used to shut down the THC would cause a large direct sea level change, masking the thermal contribution that we are interested in. Similarly, Levermann et al. (2005) exclude the direct effect of their freshwater perturbation on sea level. Land ice masses in HadCM3 are fixed, but we calculated the melt or growth of the Greenland and Antarctic ice sheets using estimated mass-balance sensitivities to local temperature change (Church et al. 2001). Expressed as equivalent sea-level rise the contributions are +0.3 mm/year per degree local warming for Greenland, and −0.4 mm/year per degree local warming for Antarctica. Change in the mass balance of 100 smaller glaciated regions was calculated as in Gregory and Oerlemans (1998). This method uses local seasonal temperature change and a time-independent mass balance sensitivity to estimate the rates of melt and accumulation. The sensitivity varies according to local conditions, but is always negative for warm anomalies. Finally, dynamical sea level height is calculated from the model's rigid lid pressure and the atmospheric pressure at sea level (which has an effect on local sea-surface height through the inverse barometer effect).

References

Allen MR, Ingram WJ (2002) Constraints on future changes in climate and the hydrologic cycle. Nature 419:224–232

Church JA, Gregory JM, Huybrechts P, Kuhn M, Lambeck K, Nhuan MT, Qin D, Woodworth PL (2001) Changes in sea level. In: Houghton JT, Ding Y, Griggs DJ, Noguer M, van der Linden P, Dai X, Maskell K, Johnson CI (eds) Climate change 2001: The scientific basis. Contribution of Working Group I to the Third Assessment Report of the Intergovernmental Panel on Climate Change. Cambridge University Press, pp. 639–693

Cox PM, Betts RA, Bunton CB, Essery RLH, Rowntree PR, Smith J (1999) The impact of new land surface physics on the GCM simulation of climate and climate sensitivity. Clim Dyn 15:183–203

Cubasch U, Meehl GA, Boer GJ, Stouffer RJ, Dix M, Noda A, Senior CA, Raper SCB, Yap KS (2001) Projections of future climate change. In: Houghton JT, Ding Y, Griggs DJ, Noguer M, van der Linden P, Dai X, Maskell K, Johnson CI (eds) Climate change 2001: The scientific basis. Contribution of Working Group I to the Third Assessment Report of the Intergovernmental Panel on Climate Change. Cambridge University Press, pp. 525–582

Curry R, Mauritzen C (2005) Dilution of the northern North Atlantic ocean in recent decades. Science 308:1772–1774

Dixon KW, Delworth TL, Spelman MJ, Stouffer RJ (1999) The influence of transient surface fluxes on North Atlantic overturning in a coupled GCM climate change experiment. Geophys Res Lett 26(17):2749–2752

Ganachaud A, Wunsch C (2000) The oceanic meridional overturning circulation, mixing, bottom water formation, and heat transport. Nature 408:453–457

Gordon C, Cooper C, Senior CA, Banks H, Gregory JM, Johns TC, Mitchell JFB, Wood RA (2000) The Simulation of SST, sea ice extents and ocean heat transports in a version of the Hadley Centre coupled model without flux adjustments. Clim Dyn 16:147–168

Gregory JM (1993) Sea level changes under increasing atmospheric CO_2 in a transient coupled ocean–atmosphere GCM experiment. J Climate 6:2247–2262

Gregory JM, Dixon KW, Stouffer RJ, Weaver AJ, Driesschaert E, Eby M, Fichefet T, Hasumi H, Hu A, Jungclaus JH, Kamenkovich IV, Levermann A, Montoya M, Murakami S, Nawrath S, Oka A, Sokolov AP, Thorpe RB (2005) A model intercomparison of changes in the Atlantic thermohaline circulation in response to increasing atmospheric CO_2 concentration. Geophys Res Lett 32:L12703

Gregory JM, Lowe JA (2000) Predictions of global and regional sea-level rise using AOGCMs with and without flux adjustment. Geophys Res Lett 27:3069–3072

Gregory JM, Oerlemans J (1998) Simulated future sea-level rise due to glacier melt based on regionally and seasonally resolved temperature changes. Nature 391:474–476

Gregory JM, Saenko OA, Weaver AJ (2003) The role of the Atlantic freshwater balance in the hysteresis of the meridional overturning circulation. Clim Dyn 21:707–717

Hulme M (2003) Abrupt climate change: can society cope? Philos Trans R Soc London 361:2001–2021

Jacob D, Goettel H, Jungclaus J, Muskulus M, Podzun R, Marotzke J (2005) Slowdown of the thermohaline circulation causes enhanced maritime climate influence and snow cover over Europe. Geophys Res Lett 32, doi:10.1029/2005GL023831

Johns TC, Gregory JM, Ingram WJ, Johnson CE, Jones A, Lowe JA, Mitchell JFB, Roberts DL, Sexton DMH, Stevenson DS, Tett SFB, Woodage MJ (2003) Anthropogenic climate change for 1860 to 2100 simulated with the HadCM3 model under updated emissions scenarios. Clim Dyn 20:583–612

Knutti R, Stocker TF (2000) Influence of the thermohaline circulation on projected sea level rise. J Climate 13:1997–2001

Latif M, Roeckner E, Mikolajewicz U, Voss R (2000) Tropical Stabilisation of the thermohaline circulation in a greenhouse warming simulation. J Climate 13:1809–1813

Levermann A, Griesel A, Hofmann M, Montoya M, Rahmstorf S (2005) Dynamic sea level changes following changes in the thermohaline circulation. Clim Dyn 24:347–354

Manabe S, Stouffer RJ (1999) The role of the thermohaline circulation in climate. Tellus 51:91–109

Marsh R, Yool A, Lenton TM, Gulamali MY, Edwards NR, Shepherd JG, Krznaric M, Newhouse S, Cox SJ (2004) Bistability of the thermohaline circulation identified through comprehensive 2-parameter sweeps of an efficient climate model. Clim Dyn 23:761–777

McInerney D, Keller K (2007) What are reliable risk-reduction strategies in the face of uncertain climate thresholds? Climatic Change, DOI 10.1007/s10584-006-9137-z, this issue

Mikolajewicz U, Voss R (2000) The role of the individual air-sea flux components in CO_2-induced changes of the ocean's circulation and climate. Clim Dyn 16:627–642

Murphy JM, Sexton DMH, Barnett DN, Jones GS, Webb MJ, Collins M, Stainforth DA (2004) Quantification of modelling uncertainties in a large ensemble of climate change simulations. Nature 430:768–772

Parker DE, Legg TP, Folland CK (1992) A new daily Central England Temperature series. Int J Climatol 12:317–342

Pope VD, Gallani ML, Rowntree PR, Stratton RA (2000) The impact of new physical parametrizations in the Hadley Centre climate model—HadAM3. Clim Dyn 16:123–146

Rahmstorf S (1996) On the freshwater forcing and transport of the Atlantic thermohaline circulation. Clim Dyn 12:799–811

Rahmstorf S (2002) Ocean circulation and climate during the past 120,000 years. Nature 419:207–214

Rahmstorf S, Ganapolski A (1999) Long-term global warming scenarios computed with an efficient coupled climate model. Clim Change 43:353–367

Rowell D, Jones R (2006) Causes and uncertainty of future summer drying over Europe. in press Clim Dyn 27:281–297

Schmittner A, Latif M, Schneider B (2005) Model projections of the North Atlantic thermohaline circulation for the 21st century assessed by observations. Geophys Res Lett 32(L23710)

Stainforth DA, Aina T, Christensen C, Collins M, Frame DJ, Kettleborough JA, Knight S, Martin A, Murphy J, Piani C, Sexton D, Smith LA, Spicer RA, Thorpe AJ, Allen MR (2005) Uncertainty in predictions of the climate response to rising levels of greenhouse gases. Nature 433:403–406

Stouffer RJ, Manabe S (2003) Equilibrium response of thermohaline circulation to large changes in atmospheric CO_2 concentration. Clim Dyn 20:759–773

Thorpe RB, Gregory JM, Johns TC, Wood RA, Mitchell JFB (2001) Mechanisms determining the Atlantic thermohaline circulation response to greenhouse gas forcing in a non-flux-adjusted coupled climate model. J Climate 14:3102–3116

Vellinga M, Wood RA (2002) Global climatic impacts of a collapse of the Atlantic thermohaline circulation. Clim Change 54(3):251–267

Vellinga M, Wood RA, Gregory JM (2002) Processes governing the recovery of a perturbed thermohaline circulation in HadCM3. J Climate 15(7):764–780

Vellinga M, Wu P (2004) Low-latitude fresh water influence on centennial variability of the thermohaline circulation. J Climate 17(23):4498–4511

Wood RA, Collins M, Gregory J, Harris G, Vellinga M (2006) Towards a risk assessment for shutdown of the Atlantic thermohaline circulation. In: Avoiding dangerous climate change, Schellnhuber HJ, Cramer W, Nakicenovic N, Wigley T, Yohe G (eds) 6:47–54

Wood RA, Keen AB, Mitchell JFB, Gregory JM (1999) Changing spatial structure of the thermohaline circulation in response to atmospheric CO_2 forcing in a climate model. Nature 399:572–575

Wood RA, Vellinga M, Thorpe RB (2003) Global warming and thermohaline circulation stability. Philos Trans R Soc London 361:1961–1975